Mass Spectrometric Identification of Novel Lysine Acetylation Sites in Huntingtin*[S]

Xin Cong‡, Jason M. Held‡, Francesco DeGiacomo‡, Akilah Bonner‡, Jan Marie Chen‡, Birgit Schilling‡, Gregg A. Czerwieniec‡, Bradford W. Gibson‡§, and Lisa M. Ellerby‡§

Huntingtin (Htt) is a protein with a polyglutamine stretch in the N-terminus and expansion of the polyglutamine stretch causes Huntington's disease (HD). Htt is a multiple domain protein whose function has not been well characterized. Previous reports have shown, however, that post-translational modifications of Htt such as phosphorylation and acetylation modulate mutant Htt toxicity, localization, and vesicular trafficking. Lysine acetylation of Htt is of particular importance in HD as this modification regulates disease progression and toxicity. Treatment of mouse models with histone deacetylase inhibitors ameliorates HD-like symptoms and alterations in acetylation of Htt promotes clearance of the protein. Given the importance of acetylation in HD and other diseases, we focused on the systematic identification of lysine acetylation sites in Htt23Q (1–612) in a cell culture model using mass spectrometry. Myc-tagged Htt23Q (1–612) overexpressed in the HEK 293T cell line was immunoprecipitated, separated by SDS-PAGE, digested and subjected to high performance liquid chromatography tandem MS analysis. Five lysine acetylation sites were identified, including three novel sites Lys-178, Lys-236, Lys-345 and two previously described sites Lys-9 and Lys-444. Antibodies specific to three of the Htt acetylation sites were produced and confirmed the acetylation sites in Htt. A multiple reaction monitoring MS assay was developed to compare quantitatively the Lys-178 acetylation level between wild-type Htt23Q and mutant Htt148Q (1–612). This report represents the first comprehensive mapping of lysine acetylation sites in N-terminal region of Htt. ***Molecular & Cellular Proteomics 10: 10.1074/mcp. M111.009829, 1–13, 2011.***

Huntington's disease (HD)[1] is a hereditary neurodegenerative disorder characterized by unrestrained movements, emotional disturbances, and psychological deterioration (1). HD patients suffer neuronal degeneration in the striatum and frontal and temporal cortex (2). HD is caused by the expansion of a polyglutamine (polyQ) stretch within the huntingtin protein (Htt). Under normal conditions, Htt is a protein with a polyQ stretch containing 2–34 repeats whereas the disease form of Htt has a polyQ repeat length longer than 36–37. Mechanisms of toxicity for mutant Htt include proteolytic cleavage by proteases such as caspase to produce toxic fragments, impaired vesicular transport, and altered transcription by binding with specific transcription coactivators and transcription factors (3–13).

Previous studies show that Htt undergoes post-translational modifications (PTMs), which are associated with alterations in localization or conformation of Htt and regulate mutant Htt toxicity (14–17). For example, phosphorylation of Htt at Ser-421 by protein kinase Akt1 can protect striatal neurons against mutant Htt-induced toxicity (18). We previously completed an analysis by MS of the phosphorylation of full-length Htt identifying numerous phosphorylation sites throughout the 3144 amino acid sequence of Htt. One of the sites was the phosphorylation at Ser-536, which blocked Htt calpain proteolysis and toxicity (14, 19, 20). In addition, lack of phosphorylation at serine-1181 Ser-1181 and Ser-1201 and serine-1201 by cyclin-dependent kinase 5 (Cdk5) leads to toxicity and accelerated neuron death (21, 22). Other PTMs such as SUMOylation (23) and ubiquitination (24) occur in Htt and alter cellular toxicity and turnover.

Acetylation is a covalent reaction in which an acetyl group is introduced to the free amino group of the protein N-terminus or the ε-amino group of lysine residues. Similar to phosphorylation, acetylation is reversible and highly regulated by histone acetyltransferases and histone deacetylases (HDACs) (25–28). Because lysine acetylation in proteins is involved in many biological functions including transcriptional regulation (29–31), apoptosis (32–34), energy metabolism (35), and DNA-related activities (36–44), there is increasing interest in exploring protein acetylation *in vitro* and *in vivo*. As compared with phosphorylation, lysine acetylation of substrates in mammalian systems generally have less specificity for the residues surrounding acetyllysine residues making predictions of acetylation sites less reliable (35, 45). To date the only estab-

From the ‡Buck Institute for Research on Aging, Novato, CA 94945
Received March 22, 2011, and in revised form, June 2, 2011
Published, MCP Papers in Press, June 18, 2011, DOI 10.1074/mcp.M111.009829

[1] The abbreviations used are: HD, Huntington Disease; Htt, huntingtin; PolyQ, polyglutamine; PTM, post-translational modification; HDAC, Histone deacetylase; LC, liquid chromatography; ESI, electrospray ionization; MRM, multiple reaction monitoring; CID, collision induced dissociation.

lished preferences are that mitochondrial substrates with histidine and tyrosine at the +1 position and sites found on protein surfaces (35, 45). Thus, the identification of acetylation sites in proteins requires analytical techniques such as MS.

Imbalance in protein acetylation is particularly relevant to a wide range of neurodegenerative diseases including HD and modulating acetylation levels represents a therapeutic target for treatment of these diseases. For example, treatment with HDAC inhibitors improves neurological performance and attenuates disease phenotypes in mouse models of polyglutamine expansion diseases including HD, amyotrophic lateral sclerosis, and Parkinson disease (46–51). The proposed mechanism for this therapeutic benefit is through correction of transcriptional dysregulation via altered histone acetylation. However, additional mechanisms such as changes in the acetylation status of the Huntington's disease protein Htt itself or other protein targets may be relevant.

Different technologies have been applied to the discovery of lysine acetylation in proteins. Radiolabeling and immunodetection are among the most popular methods and have facilitated identification of many acetylated proteins (52–55). However, neither approach provides information on the number and exact site of acetylation. In recent years, mass spectrometry has become a powerful tool in detecting protein PTMs including acetylation (56–62). Acetylated peptides can be distinguished from their unmodified forms by a characteristic mass shift of +42.0106 Da, although trimethylation of lysines has a similar mass shift of +42.0470 Da. Tandem mass spectrometry provides sequence information and can locate the acetylation sites. Moreover, tandem mass spectra of acetylated peptides reveal highly specific immonium ions at *m/z* 143.1 and 126.1 that can be used as "reporter" ions indicating acetylated lysine residues (8, 63–65) as well as differentiating this modification from trimethylation (66). The application of mass spectrometry can also accelerate the analysis of lysine acetylation. Previous mass spectrometric analyses have in part focused on specific target proteins, such as histones (67, 68) and p53 (69). But recently lysine acetylation studies have been extended to investigate diverse cellular proteins (45, 70) and whole organism proteomes (35).

Here we report mass spectrometric analysis of acetyllysine in a disease-relevant truncated N-terminal form of Htt. Myc-tagged Htt23Q (with a polyQ length of 23) and Htt148Q (with an expanded polyQ length of 148) containing amino acids 1–612 were immunoprecipitated from mammalian cell lysates, and subjected to nano-liquid chromatography-electrospray ionization tandem MS (LC-ESI-MS/MS) analyses after in-solution digestion with several proteases. In all, five lysine acetylation sites of Htt23Q (1–612) and Htt148Q (1–612) were identified by MS/MS in this study and antibodies against these sites were generated. Further, a multiple reaction monitoring (MRM) MS method was developed to compare the Lys-178 acetylation levels between wild-type Htt23Q and mutant Htt148Q (1–612).

EXPERIMENTAL PROCEDURES

Site-directed Mutagenesis—Site-directed mutagenesis of the Htt constructs pTet-c-Myc-Htt23Q and pTet-c-Myc-Htt148Q (20) was performed using the QuikChange kit (Stratagene, La Jolla, CA) using the following primers: a double stop was inserted after amino acid 612, forward, 5′-CCACAGGTA-TTCTTCCTTAGTAAG-CCTCGGAG-GCCTTCAGG-3′, reverse, 5′-CCTGAAGGCC-TCCGAGGCTTAC-TAA-GGAAGAATACCTGTGG-3′. PCR was performed using 15 or 25 ng of DNA, 5 μl of 10X *Pfu* buffer (Stratagene), 2.5 μl of dimethyl sulfoxide, 0.2 mM dNTPs (Roche Molecular Biochemicals), 125 ng each of forward and reverse primers (Integrated DNA Technologies, Coralville, IA), 3 μl of Quick Change Solution (Stratagene), and 1 μl *Pfu* Turbo Polymerase (Stratagene) at 95 °C for 1 min, 16 cycles at 96 °C for 50s, 55 °C for 1 min, and 65 or 68 °C for 45 min, and 68 °C for 10 min. Plasmids were DpnI (Stratagene)-treated, transformed into XL1-Blue Supercompetent cells (Stratagene), and purified using the Qiagen Plasmid Mini Kit. Mutations, CAG repeat length, and construct integrity were confirmed by DNA sequencing. Mutated constructs of pTet-c-myc-Htt23Q (1–612) and pTet-c-myc-Htt148Q (1–612) with the stop codon after amino acid 612 were used for these studies.

Cell Culture and Transfection—HEK 293T cells were grown in Dulbecco's modified Eagle's medium with 10% fetal bovine serum. Htt constructs pTet-c-myc-Htt23Q (1–612), pTet-c-myc-Htt148Q (1–612), Htt15Q (1–1212), Htt138Q (1–1212), or vector control were transfected into HEK 293T cells with Superfect (Qiagen, Valencia, CA) according to the manufacturer's instructions (4). Serum was withdrawn from the medium 24 h before harvesting to reduce protein contamination for mass spectrometric analysis. The cells were treated with a HDAC inhibitor mixture containing 50 μM trichostatin A (from a 50 mM stock solution in ethanol, Sigma); 30 μM sodium butyrate (from a 55 mM aqueous stock solution, Sigma) and 30 mM nicotinamide (from a 1 M aqueous solution, Sigma) for 4 h before harvesting. The HDAC treated cells were harvested 48 h after transfection.

Immunoprecipitation and Western Blot Analysis—Harvested cells were lysed with Mammalian Protein Extraction Reagent (M-PER, Pierce) lysis buffer with protease inhibitors (Mini Complete, Roche) and HDAC inhibitors as described above. Lysates were sonicated 5 times with a 3-s pulse and spun at 16000 × *g* for 20 min to remove debris. Protein concentration was determined with BCA Protein Assay Kit (Pierce). HEK 293T cell lysates with either c-myc-Htt23Q (1–612), pTet-c-myc-Htt148Q (1–612), or vector control were incubated with immobilized anti-c-Myc agarose beads (Pierce) overnight. The beads were washed with Tris-buffered saline/Tween 20 (TBST) (25 mM Tris, 0.15 M NaCl, pH 7.2 + 0.05% Tween-20, Pierce) and 10 mM Tris, pH 7.4, respectively. Htt was eluted with M-PER buffer containing 10 mg/ml c-Myc peptide (Anaspec), 200 mM NaCl and 0.1% Nonidet P-40 (Sigma). Immunoprecipitated samples were dialyzed in TBST and 25 mM NH_4HCO_3 sequentially, and then applied to a clean-up procedure using a two-dimensional clean-up kit (Amersham Biosciences). The resulting pellet was dissolved in appropriate amount of SDS-PAGE loading buffer, depending on the size of the pellet, and run on a NuPAGE 4–12% BisTris gel (Invitrogen, Carlsbad, CA) in 3-(*N*-morpholino)propanesulfonic acid (MOPS) running buffer (Invitrogen) for 80 min at 200V. Typically 10% of the sample was used for Western blotting and the rest of the sample was used for mass spectrometric analysis.

Custom antibodies (Open Biosystems) were produced by injecting synthesized peptides (supplemental Table S1) corresponding to the acetylated lysine sites into rabbits. The day 58 postimmunization bleeds were collected. Serum was tested for signal by Western blots. Those with positive results were purified by affinity binding using immobilized peptides (supplemental Table S1) and stored for use.

In-gel Proteolytic Digestion—Bands containing Htt were excised from the one-dimensional SDS-PAGE gels and subsequently

destained and dehydrated with acetonitrile. For trypsin and Asp-N digestion, proteins were reduced with 10 mM dithiothreitol (Sigma) in 25 mM NH_4HCO_3 at 56 °C for 1 h and alkylated with 55 mM iodoacetamide (Sigma) in 25 mM NH_4HCO_3 at room temperature for 45 min. The samples were then incubated with 100–200 ng sequencing grade trypsin (Promega) or Asp-N (Roche) at 37 °C for 16–18 h. For the chymotrypsin (Roche) digestion, dithiothreitol was dissolved in a 25 mM NH_4HCO_3 solution containing 4 M guanidine hydrochloride (Sigma) in the reduction/denaturation step. After alkylation, the samples were incubated with 100–125 ng chymotrypsin at 25 °C for 16–18 h. The peptides were subjected to aqueous extraction (H_2O) and hydrophobic extraction (50% acetonitrile, 5% formic acid) and concentrated under vacuum to a 10–15 μl final volume.

Quadrupole Time-of-Flight Mass Spectrometric Analysis of Peptides—Mass spectra of peptides generated after proteolytic digestion of Htt were acquired by reverse-phase nano-high performance liquid chromatography (HPLC)-ESI-MS/MS using an Eksigent nano-LC two-dimensional HPLC system (Eksigent, Dublin, CA) that was directly connected to a quadrupole time-of-flight (QqTOF) QSTAR Elite mass spectrometer (AB SCIEX, Concord, Canada). Briefly, an aliquot of digested peptide mixture (~2 μl at a concentration of 1 μg/μl) was loaded onto a guard column (C18 Acclaim PepMap100, 300 μm I.D. × 5 mm, 5 μm particle size, 100 Å pore size; Dionex, Sunnyvale, CA) and washed with the loading solvent (98% solvent A, 2% solvent B, flow rate: 20 μl/min) for 5 min where solvent A consisted of 0.1% formic acid in 98% H_2O, 2% acetonitrile and solvent B consisted of 0.1% formic acid in 98% acetonitrile, 2% H_2O. Subsequently, samples were transferred onto the C18-nanocapillary HPLC column (C18 Acclaim PepMap100, 75 μm I.D. × 15 cm, 3 μm particle size, 100 Å pore size; Dionex) and eluted at a flow rate of 300 nL/min using the following gradient: 2–40% solvent B in A (from 0 to 35 min), 40–80% solvent B in A (from 35 to 45 min) and at 80% solvent B in A (from 45 to 55 min), with a total run time of 95 min (including mobile phase equilibration). In some experiments, another gradient was applied: 2–30% solvent B in A (from 0 to 30 min), 30–80% solvent B in A (from 30 to 35 min) and at 80% solvent B in A (from 35 to 39 min), with a total runtime of 60 min (including mobile phase equilibration). Mass spectra (ESI-MS) and tandem mass spectra (ESI-MS/MS) were recorded in positive-ion mode with a resolution of 12,000–15,000 full-width half-maximum. Data acquisition was performed with an ion spray voltage of 2300 V, curtain gas of 20 psi, ion source gas of 17 psi, and an interface heater temperature of 100°C. A declustering potential of 65 and focusing potential of 275. For collision induced dissociation tandem mass spectrometry (CID-MS/MS), the mass window for precursor ion selection of the quadrupole mass analyzer was set to ± 1 *m/z*. The precursor ions were fragmented in a collision cell using nitrogen as the collision gas. A CAD gas setting of 5 was applied. Information dependent acquisition was used for MS/MS collection, including QSTAR Elite (Analyst QS 2.0) specific features, such as "Smart Collision" and "Smart Exit" (fragment intensity multiplier set to 6.0 or 8.0 and maximum accumulation time at 2 or 2.5 s) to obtain MS/MS spectra for the four most abundant precursor ions after each MS survey scan. For selected experiments, the Q2 transmission windows were adjusted (supplemental Table S2) and the software feature "use iTRAQ reagent" option was chosen to improve detection of low mass immonium ion region and adjust collision energy in the MS/MS spectra.

LC-MRM/MS—Samples were analyzed by nano-LC-MRM/MS on a 4000 QTRAP hybrid triple quadrupole/linear ion trap mass spectrometer (AB SCIEX, Concord, Canada). Chromatography was performed using a NanoLC-2D LC system (Eksigent, Dublin, CA) with aqueous buffer A (0.1% formic acid) and buffer B (90% acetonitrile in 0.1% formic acid). Digestion mixtures were loaded at 20 μl/min (0.1% formic acid) onto a 5 mm × 300 μm reversed phase C18 trap column (5 μm, 100Å) (Dionex, Sunnyvale, CA) and eluted at 300 nL/min with a gradient of 2–70% B over 32 min using with a 75 μm inner diameter Integrafrit analytical column (New Objective, Woburn, MA) packed in-house with 10–12 cm of ReproSil-Pur C18-AQ 3 μm reversed phase resin (Dr. Maisch GmbH, Germany). Peptides were ionized using a PicoTip emitter (75 μm, 15 μm tip; New Objective). Data acquisition was performed using Analyst 1.5 (ABSciex) with an ion spray voltage of 2450 V, curtain gas of 10 psi, nebulizer gas of 20 psi, and an interface heater temperature of 150°C. The transitions, dwell times, and collision energies are listed in supplemental Table S3. A declustering potential of 70 was used for all transitions. MRM transitions were monitored and acquired at unit resolution both in the first and third quadrupoles (Q1 and Q3). MultiQuant version 1.1 (ABSciex) was used to process all MRM data. Each transition was individually integrated to generate peak areas. If a peak was not detected, the level of background was integrated. To quantify acetylated Lys-178 by MRM a custom stable isotope labeled peptide was synthesized, $EIKK_{ac}NGAP^*R$ in which the proline (P*) was labeled with five ^{13}C and one ^{15}N (Anaspec) and was used as an internal standard.

Database Searches—Mass spectrometric data were analyzed with an in-house licensed bioinformatics database search engine system Mascot version 2.2.04 (Matrix Sciences, London, UK) (71). Peaklists for the QSTAR Elite LC-MS/MS data sets were generated using the Mascot.dll script version 1.6b19 for Analyst QS 2.0 (parameters used: remove peaks with intensity less than 0.1% of the highest peak; centroid all MS/MS data, merge distance 0.02). Files were submitted to the Mascot search engine using Mascot Daemon version 2.2.2. Mascot uses a probability based "Mowse Score" to evaluate data obtained from tandem mass spectra. The following search parameters were used: enzyme specificity was defined as trypsin with two possible missed cleavages, carbamidomethyl (Cys) was chosen as fixed modification, acetyl (Protein N-terminal), Gln->pyro-Glu (N-terminal Gln), and oxidation (Met) were chosen as variable modifications, mass tolerance for precursor ions was 50 ppm, mass tolerance for fragment ions was 0.4 Da. The publicly available SwissProt database release version 56.2 (release 23-Sep-2008) was searched for most data obtained from human samples with species restriction "human" (20407 sequences); Ions scores are [-10*Log(P)], where P is the probability that the observed match is a random event. For human Mascot database searches, a cut-off expectation value of 0.02 (significance threshold) was chosen for individual MS/MS spectra, which resulted in a false discovery rate of 3.09% (automatic decoy database search) (supplemental Table S4). For acetyllysine identification, all data sets were also searched using the Mascot in-house search engine against a custom database representing Htt protein spanning residues 1–612 fused to an N-terminal myc tag peptide. The following search parameters were used: enzyme specificity was defined as trypsin, Asp-N, chymotrypsin with three possible missed cleavages (supplemental Table S5), respectively, carbamidomethyl (Cys) was chosen as fixed modification, acetyl (Lys), acetyl (Protein N-terminal), Gln->pyro-Glu (N-terminal Gln), and oxidation (Met) were chosen as variable modifications, mass tolerance for precursor ions was 0.4 Da, mass tolerance for fragment ions was 0.4 Da.

RESULTS

Immunoprecipitation of Htt—To purify Htt for MS analysis, myc-Htt23Q (1–612) and myc-Htt148Q (1–612) was overexpressed in 293T cells and immunoprecipitated in the presence of HDAC inhibitors. As shown in Fig. 1*A*, Western blot analysis of lysates (input before incubation with immobilized anti-c-Myc antibody) and flow through (supernatant after incubation with immobilized anti-c-Myc antibody) demonstrate depletion of Htt with c-Myc beads. Complete depletion of Htt from the

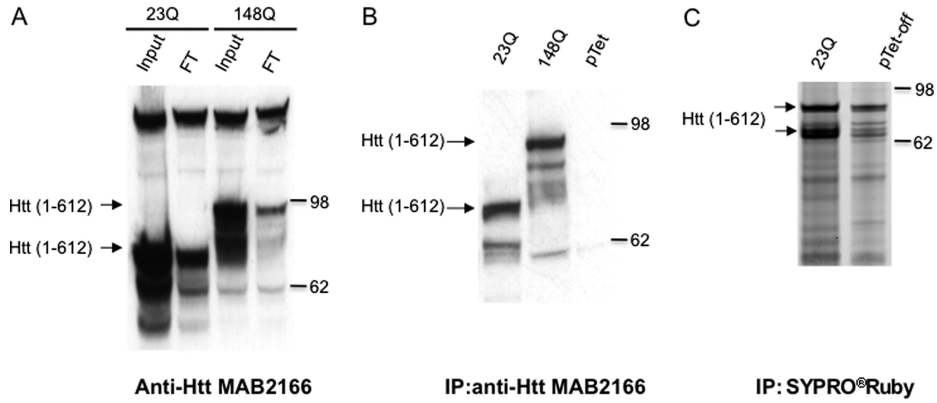

FIG. 1. **Immunoprecipitation and Western blot analysis of Htt.** Myc-tagged Htt (1–612) constructs (23Q and 148Q) were expressed in 293T cells. *A*, Lysate input and flow-through (FT) during the immunoprecipitation procedure and (*B*) Immunoprecipitated Htt were probed with monoclonal N-terminal Htt antibody 2166. *C*, Immunoprecipitation and 1D SDS-PAGE of expressed Htt stained with Sypro Ruby. Myc-tagged Htt23Q (1–612) expressed in 293T cells was immunoprecipitated from cellular lysates using the Pierce Profound Mammalian C-myc tag IP/Co-IP kit. Samples were separated by one-dimensional SDS-PAGE on 4–12% Bis-Tris gels. Gels were stained with fluorescent SyproRuby protein gel stain (Invitrogen).

TABLE I

Summary of acetyllysine and corresponding unmodified peptides in Htt23Q (1–612) identified by HPLC-ESI-MS/MS

Peptide sequence[a]	Acetyl-Lys sites	*m/z* (obs)	M (obs)	M (calc)	ΔM (Da)	ΔM (ppm)	Mascot score[b]	Expect values[b]	Retention time(min)	Enzyme[c]
$E^{5}KLMK_{Ac}AF^{11}$	Lys-9	454.74	907.47	907.48	−0.01	−11	27	0.002148	28.04	chym
$E^{5}KLM_{ox}K_{Ac}AF^{11}$	Lys-9	462.73	923.45	923.48	−0.03	−32	33	0.00047	27.06	chym
$E^{175}IKK_{Ac}NGAPR^{183}$	Lys-178	352.2	1053.58	1053.59	−0.01	−9	34	0.00041	27.15	trypsin
$A^{231}AAVPK_{Ac}IM_{ox238}$	Lys-236	429.74	857.46	857.47	−0.01	−12	47	2.02E-05	23.09	chym
$A^{231}AAVPKIM_{ox238}$	-	408.72	815.43	815.46	−0.03	−37	46	2.43E-05	21.1	chym
$D^{333}TSLKGSFGVTRK_{Ac}EM^{347}$	Lys-345	566.61	1696.8	1696.85	−0.05	−29	75	3.16E-08	25.68	Asp-N
$D^{333}TSLKGSFGVTRK_{Ac}EM_{ox347}$	Lys-345	571.94	1712.79	1712.84	−0.05	−29	67	1.98E-07	23.4	Asp-N
$D^{333}TSLKGSFGVTRKEM_{ox347}$	-	557.94	1670.81	1670.83	−0.03	−18	31	0.0008	20.5	Asp-N
$S^{438}RKQKGK_{Ac}V^{445}$	Lys-444	486.8	971.58	971.59	−0.01	−10	31	0.00073	16.99	chym
$S^{438}RKQKGKV^{445}$	-	465.79	929.57	929.58	−0.01	−11	42	5.93E-05	15.08	chym

[a] K_{Ac}: acetylated lysine residue.

[b] Mascot 2.2.04 search engine result score searching against a custom database representing huntingtin spanning residues 1–612 fused to an N-terminal myc tag peptide stretch.

[c] chym: chymotrypsin; Asp-N: Endopeptidase Asp-N.

cell lysates was not observed because of the fact that the c-myc tag of Htt became acetylated under these conditions. c-Myc-tagged Htt in the lysates bound to the immobilized anti-c-Myc antibody. As shown in Fig. 1*B*, Western blot analysis demonstrates that Htt23Q (1–612) and Htt148Q (1–612) elutes after immunoprecipitation from 293T cells. The eluted proteins were dialyzed and precipitated to remove excess c-Myc peptide and salt. The resulting proteins were separated by one-dimensional SDS-PAGE and visualized with Sypro Ruby protein gel stain (Fig. 1*C*). Although some co-immunoprecipitated proteins have similar molecular weight as Htt, their presence did not interfere with mass spectrometry analysis.

Identification of Htt by Mass Spectrometry—The gel band containing Htt23Q (1–612) was excised and digested with trypsin, Asp-N, and chymotrypsin, respectively. The resulting peptides were separated and analyzed by nano-HPLC (reversed-phase C18 chromatography) coupled to a hybrid quadrupole time-of-flight mass spectrometer (QSTAR Elite). Peptide sequence information was provided by CID. supplemental Table S5 shows a list of all Htt peptides sequenced by nano-HPLC-ESI-MS/MS.

Acetylated Lysines Identified by Nano-HPLC-ESI-MS/MS—The ESI-MS/MS data were searched against a customized Htt (1–612) database by Mascot to identify lysine acetylation sites. Rigorous criteria were used to identify acetyllysine containing peptides to avoid false positive assignments. This became relevant after Stevens *et al.* (72) described reports of other groups that incorrectly assigned post-translationally modified peptides. Our criteria for identifying acetyl lysine modifications consisted of the following: (1) pairs of unmodified peptides and acetyllysine peptides were observed that showed similar ion series, except in a few cases where the unmodified peptides was not observed because of further cleavage at the unmodified lysine by trypsin; (2) peptides containing acetyllysine showed a increased retention time shift of 2–4 min relative to the unmodified peptide because acetylated peptides are more hydrophobic and elute later (Table I); (3) mass accuracy of the molecular ion was <50 ppm

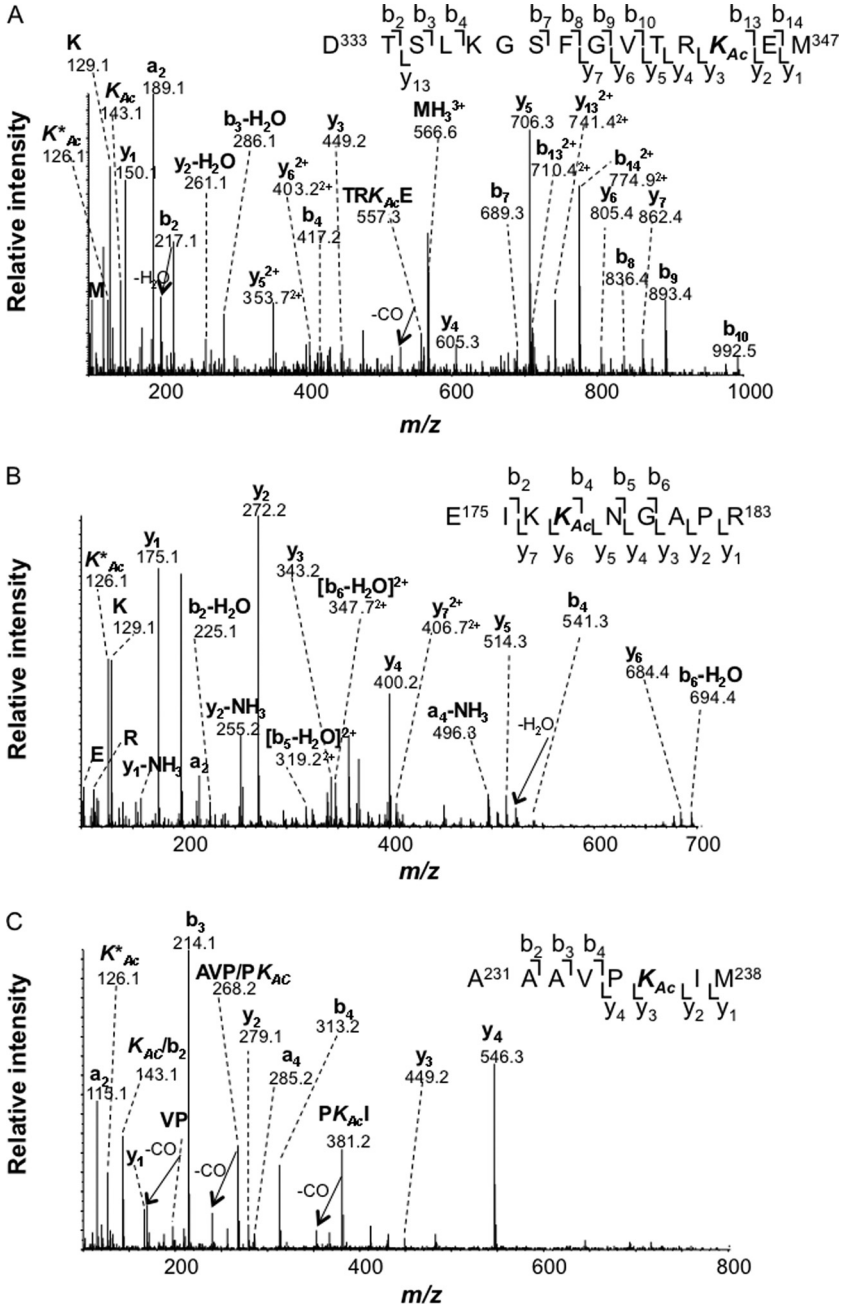

FIG. 2. **Three novel Htt acetylation sites identified by mass spectrometry.** *A*, ESI-MS/MS tandem mass spectra of Lys-acetylated peptide DTSLKGSFGVTRK$_{Ac}$EM (residues 333–347) obtained after Asp-N digestion of immunoprecipitated Htt23Q (1–612) with high (*A*) and low (*B*) collision energy. The molecular ion $[M+3H]^{3+}$ at *m/z* 566.61 (M = 1696.80) was selected for CID. *B*, ESI-MS/MS tandem mass spectra of Lys-acetylated peptide EIKK$_{Ac}$NGAPR (residue 175–183) obtained after trypsin digestion of immunoprecipitated Htt23Q (1–612). The molecular ion $[M+3H]^{3+}$ at *m/z* 352.21 (M = 1053.60) was selected for CID. *C*, ESI-MS/MS tandem mass spectra of Lys-acetylated peptide AAAVPK$_{Ac}$IM (residues 231–238) obtained after chymotrypsin digestion of immunoprecipitated Htt23Q (1–612). The molecular ion $[M+2H]^{2+}$ at *m/z* 429.73 (M = 857.44) was selected for CID. K*: In all three spectra, is the diagnostic immonium for acetyllysine at *m/z* 126.1.

for both the unmodified and acetyl lysine modified peptide; (4) MS/MS fragmentation spectra of the acetyl lysine containing peptides required the presence of y- or b- fragments that flanked the acetyl lysine residue (for more details see below), and finally; (5) peptides containing acetyllysine must show an acetyllysine immonium ions (*m/z* 126.1 and/or 143.1). These criteria ensure the accuracy of acetyllysine peptide identifications.

As shown in Table I, we identified three novel sites of lysine acetylation (Lys-178, Lys-236, and Lys-345) and two previously published sites (Lys-9 and Lys-444) (73, 74) in human Htt (1–612) from their MS/MS spectra. We found that only five of the 27 possible lysine sites in Htt23Q (1–612) were detected as acetylated in the MS/MS spectra of the Htt peptides supplemental Fig. S1. Fig. 2 illustrates the identification of the three novel lysine acetylation sites in Htt from ESI-MS/MS data. The tandem mass spectrum of acetylated lysine containing peptide DTSLKGSFGVTRK$_{Ac}$EM (residues 333–347) generated from chymotrypsin AspN digestion of Htt23Q (1–612) is shown in Fig. 2*A*. A comprehensive b-ion series and several y-ions that also flanked the acetyllysine site confirmed the presence of an acetyl group at Lys-345 as did the diagnostic acetyllysine immonium ion at *m/z* 126.1. In addition, the corresponding unmodified peptide DTSLKGSFGVTRKEM

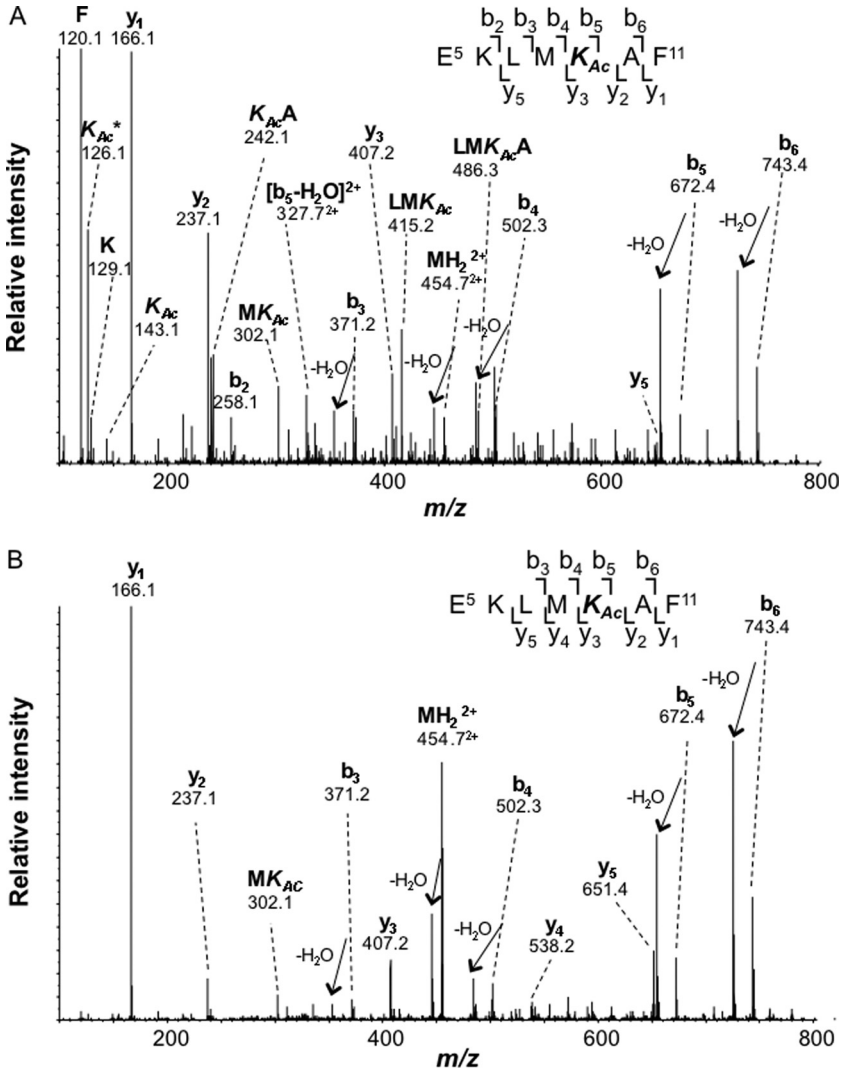

FIG. 3. **ESI-MS/MS tandem mass spectra of the acetylated lysine peptide EKLMK$_{Ac}$AF (residue 5–11) obtained after Asp-N digestion of immunoprecipitated Htt23Q (1–612).** *A*, The molecular ion $[M+2H]^{2+}$ at *m/z* 454.74 (M = 907.47 Da) was selected for CID. K* refers to the two immonium ions for acetyllysine at *m/z* 126.1 and 143 under Q2 transmission setting 1 described in supplemental Table S2. *B*, The molecular ion $[M+2H]^{2+}$ at *m/z* 454.74 (M = 907.47 Da) was selected for CID. K* refers to the two immonium ions for acetyllysine at *m/z* 126.1 and 143 under Q2 transmission setting 2 described in supplemental Table S2.

was also observed (as listed in supplemental Table S5). The pair was chromatographically separated by nearly 3 min, the hydrophobic acetylated peptide eluted at 23.40 min and the unmodified peptide at 20.67 min.

The tandem mass spectrum of acetyl lysine peptide EIKK$_{Ac}$NGAPR (residue 175–183) generated from trypsin digestion of Htt23Q (1–612) is shown in Fig. 2*B*. The b-ion series and an almost complete y-ion series that flanked the acetyl lysine site was consistent with the presence of acetyl group at Lys-178. As before, the acetyl lysine immonium ion at *m/z* 126.1 was detected as well. However, the corresponding unmodified peptide was not observed likely because of further cleavage of one of the two internal lysine residues.

Fig. 2*C* shows the ESI-MS/MS tandem mass spectra of lysine-acetylated peptide AAAVPK$_{Ac}$IM (residue 231–238) generated after chymotrypsin digestion. As in the two previous examples, several y-ions flanked the acetyl lysine site at Lys-236 and an acetyl lysine immonium ion at *m/z* 126.1 was detected. In addition, the corresponding unmodified peptide AAAVPK$_{Ac}$IM (residue 231–238) was detected in the experiment (as listed in supplemental Table S5) and also separated by nearly 3 min, with the more hydrophobic acetylated peptide eluting at 24.3 min and the unmodified peptide at 21.1 min.

Two other previously reported lysine acetylation sites, Lys-9 and Lys-444 (73, 74), were also identified using the same approach as described above (73, 74). The tandem mass spectrum of the corresponding acetyl lysine peptides encompassing these two known sites are provided in Fig. 3*A* and supplemental Fig. S2. Both b- and y-ion series flanked the acetyl lysine at Lys-9 in the chymotryptic peptide EKLMK$_{Ac}$AF (residues 5–11). The aceyllysine-specific immonium ions at *m/z* 126.1 and 143.1 also provide additional confidence for this assignment. The fragment ion series of b- and y-ions not only provides sequence information on the peptide, but also indicates the site of lysine acetylation at Lys-9 by mass shifts of an additional 42 Da for the y_3 (*m/z* 407.2) and y_5 (*m/z* 651.4) fragment ions. The fact that there is

no +42 Da mass shift for the b_2-b_4 fragments ions eliminates the possibility of acetylation at Lys-6. Last, manipulating Q2 transmission parameters when acquiring tandem mass spectra had a predictable effect on spectra quality and overall confidence in both identification of the lysine acetyl group as a PTM and the specific site of lysine acetylation.

Fig. 3 also shows the MS/MS spectra of the same peptide EKLMK$_{Ac}$AF obtained with the mass spectrometric Q2 transmission set to enhance low mass ions (Fig. 3*A*) in comparison to the Q2 transmission set to focus on medium and high mass fragment ions (Fig. 3*B*). Details for the Q2 transmission window settings can be found in supplemental Table S2. The peptide follows similar fragmentation patterns under both conditions. However, as shown in Fig. 3*B*, the most intense ions are b- and y-ion series in the medium to high mass range (above *m/z* 400). With the Q2 transmission parameter setting adjusted to favor the low mass ion region, more and higher abundance peaks were observed in the mass range below *m/z* 300 (Fig. 3A) which enhances the appearance of highly selective acetyl lysine immonium ions at *m/z* 126.1 and 143.1. Under these altered transmission conditions, some MS/MS spectra of acetyl lysine containing peptides contain immonium ions that are among the most intense peaks in the spectra, whereas few b- and y-ions were observed (data not shown).

Acetylation Antibodies to Lys-236, Lys-345 and Lys-444 Confirm Site of Acetylation—Our experiments allowed new modifications to be uncovered in Htt. To confirm the three novel acetyl lysine sites identified in our MS studies of Htt, site-specific polyclonal anti-acetyl lysine antibodies were generated to four (Lys-178, Lys-236, Lys-345, and Lys-444) of the identified Htt acetylation sites. The sera from rabbits to acetyl lysine antibody to the Htt Lys-178 site were of low titer. Western blot analysis for acetylation of Htt revealed that both wild-type and mutant Htt were acetylated at Lys-236, Lys-345, and Lys-444 (Fig. 4). As previously reported we found that mutant Htt has higher levels of acetylation at Lys-444 when compared with wild-type Htt (73). Interestingly, we observed that the level of acetylation of Htt varied in the wild-type and mutant Htt. Generally, the levels of aceylation appear to be higher in Htt138Q (1–1212) at Lys-236, Lys-345 and Lys-444 when compared with Htt15Q (1–1212). We used these constructs because they do not contain an artificial tag in the Htt protein. The production of acetyl lysine to Lys-9 was not pursued because this has been previously published (75).

Comparison of Lysine Acetylation Levels at Lys-178 in Htt23Q to Htt148Q—To study the progressive lysine acetylation in Htt, a mass spectrometry-based semiquantitative method was employed using peak area to evaluate the relative abundance of Lys-178 acetylation in wild-type and mutant Htt. We focused on this particular acetylation site for several reasons: (1) it is near the polyglutamine stretch and an identified protease cleavage site (near the polyglutamine stretch and a76, 77); (2) antibodies were not successfully

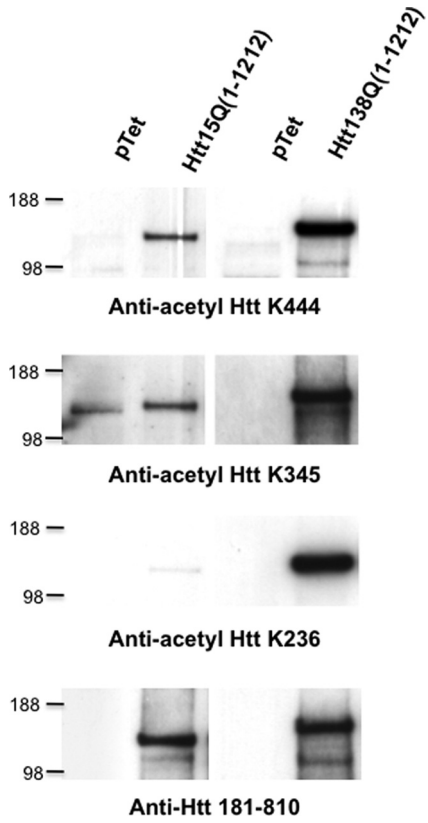

FIG. 4. **Western blot analysis of Htt with anti-acetyllysine antibodies.** Htt15Q and Htt138Q (1–1212) were expressed in 293T cells and lysates were probed with anti-acetyllysine-236, 345, 444 polyclonal antibodies and N-terminal Htt antibody 2166.

generated to this site to allow quantification; and (3) to establish mass spectrometry methods to monitor changes in acetylation quantitatively. For this analysis, Htt23Q (1–612) and Htt 148Q (1–612) were immunoprecipitated from 293T cells and the gel bands containing Htt were excised and digested with trypsin. It is important to point out that we are measuring the soluble Htt23Q and Htt148Q forms as this material migrated into the SDS-gel. Therefore our analysis reflects only the levels of acetylation in soluble Htt at Lys-178. The heavy labeled synthetic peptide containing Lys-178 was spiked in (100 fmol) and the samples were analyzed in MRM mode using a 4000 QTRAP mass spectrometer. The MRM transitions (supplemental Table S3) were derived from MS/MS data obtained as described above by ESI-MS/MS using the QqTOF platform.

For this targeted lysine-containing tryptic peptide ^{175}EIKK$_{Ac}$NGAP^{183}R, lack of acetylation causes further cleavage by trypsin and generates shorter peptides than the acetylated peptide and, therefore, were not observed. In this case, MRM transitions to six nonmodified peptides throughout the Htt sequence were used to normalize for quantitation supplemental Fig. S5. A heavy isotope-labeled synthetic peptide corresponding to the targeted acetyl lysine-containing peptide was employed to validate the method. When spiked

TABLE II
Comparison of acetylated lysine levels at Lys-178 in Htt23Q (1–612) and Htt148Q (1–612) using MRM-MS quantitation

Biological replicates	Peak area[a]		Htt 23Q/148Q ratio		
	23Q	148Q	Fold change of acetyl K178	Total Htt[b]	Normalized fold change of acetyl K178[c,e]
1	182527	62700	2.9	0.89	3.3
2	166802	51498	3.2	0.89	3.6
3	114802	32163	3.6	0.97	3.7
4	79483	27854	2.9	0.96	3.0
5	384157	235079	1.6	0.65	2.5
6	665288	51899	12.8	0.99	12.9
					4.8 ± 4.0[d] Average ± standard deviation

[a] Extracted ion chromatogram peak area of MRM transition 352.2(Q1)/272.2(Q3) for the acetyl peptide ^{175}EIKK$_{Ac}$NGAP^{183}R.
[b] The relative Htt levels were obtained from non-K178-containing peptides. More detail is displayed in supplemental methods.
[c] The fold change in 23Q/148Q fold normalized of total Htt.
[d] Using Wilcoxon signed rank test with a two-tailed test to evaluated statistical significance we found a $p^* < 0.03$ for Htt23Q compared to Htt148Q.
[e] Normalization is described in detail in the supplemental materials.

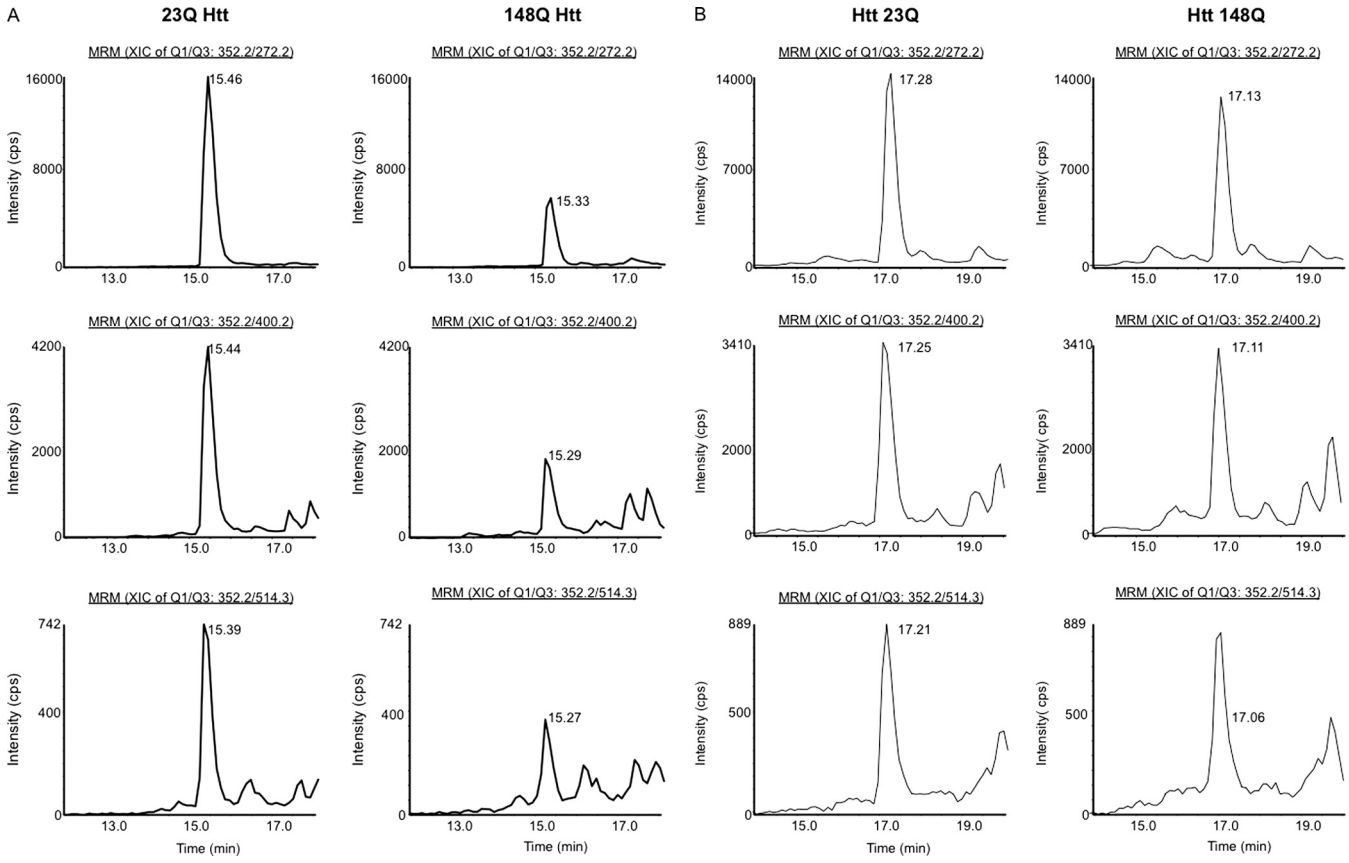

FIG. 5. **Representative MRM extracted ion chromatograms (XIC) for wild type (Htt23Q) and mutant (Htt148Q) peptide.** *A*, MRM extracted ion chromatograms (XIC) for wild type (Htt23Q) and mutant (Htt148Q) peptide ^{175}EIKK$_{Ac}$NGAP^{183}R containing Lys-178 for each transition. Three transitions were selected for our analysis as depicted by the three panels. This was used in our quantitative analysis of the ratio of Htt23Q to Htt148Q. *B*, MRM extracted ion chromatograms (XIC) for wild-type (Htt23Q) and mutant (Htt148Q) peptide ^{175}EIKK$_{Ac}$NGAP^{183}R containing Lys-178 for each transition in the presence of HDAC inhibitors.

in the digested Htt samples, the synthetic peptide EIKK$_{Ac}$NGAP*R (where P* is $^{13}C_5{}^{15}N_1$-proline) elutes at the same retention time as the endogenous peptide ^{175}EIKK$_{Ac}$NGAP^{183}R. (supplemental Fig. S3). Moreover, the MS/MS spectrum of peptide ^{175}EIKK$_{Ac}$NGAP^{183}R obtained by the QqTOF mass spectrometer and the hybrid triple quadrupole/linear ion trap mass spectrometer (4000 QTRAP) show very similar fragmentation patterns (supplemental Fig. S4). A preparation of six biological replicates were purified for both Htt23Q (1–612) and Htt148Q (1–612), and these were analyzed using the semiquantitative LC-MRM-MS assay described above, targeting specifically the

TABLE III
Quantitation of acetylated lysine levels at Lys-178 in Htt23Q (1–612) and Htt148Q (1–612) in the presence of HDAC inhibitors

Biological replicates	Peak area[a]		Htt 23Q/148Q ratio		
	23Q	148Q	Fold change of acetyl K178	Total Httb[b]	Normalized fold change of acetyl K178[c,e]
1	393530	218286	1.8	1.3	1.4
2	164565	109927	1.5	1.3	1.1
3	306265	138232	2.2	1.5	1.5
					1.3 ± 0.18[d] Average ± standard deviation

[a] Extracted ion chromatogram peak area of MRM transition 352.2(Q1)/272.2(Q3) for the acetyllysine peptide ^{175}EIKK$_{Ac}$NGAP^{183}R.
[b] The relative Htt levels were obtained from non-K178-containing peptides. More detail is displayed in supplemental methods.
[c] The fold change in 23Q/148Q fold normalized of total Htt.
[d] Using Wilcoxon signed rank test with a two-tailed test to evaluated statistical significance we found a $p^* < 0.1443$ for Htt23Q compared to Htt148Q.
[e] Normalization is described in detail in the supplemental materials.

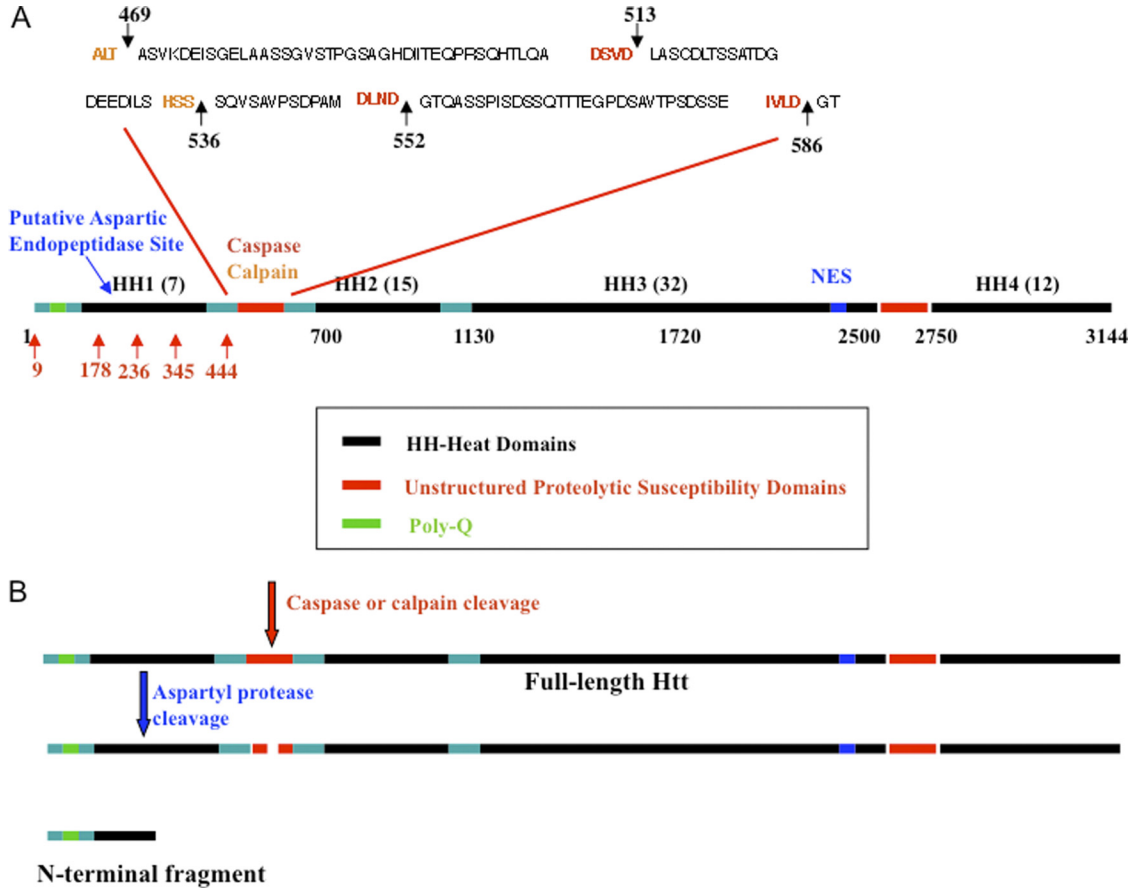

FIG. 6. **Summary scheme of Htt PTMs.** *A*, Schematic of Htt structure with four HEAT repeat domains (HH) and caspase/calpain domain. Red *arrows* indicate lysine acetylation sites identified by MS/MS in this study. *B*, N-terminal fragment of mutant Htt has enhanced toxicity.

^{175}EIKK$_{Ac}$NGAP^{183}R. Lys-178 acetylation levels from Htt23Q and Htt148Q and comparison after normalization to overall Htt protein abundance as shown in Table II.

In Fig. 5*A*, the representative extracted ion chromatograms (XIC) of the purified Htt23Q (1–612) and Htt148Q (1–612) are shown for three MRM transitions. Using MRM analysis, the level of acetylated lysine at Lys-178 in Htt23Q (1–612) is 4.83-fold higher than in the Htt148Q protein (Table II). Using the Wilcoxon signed rank test with a two-tailed test to evaluated statistical significance we found a $p^* < 0.03$. We conclude the increase in acetylated Lys-178 in the wild-type Htt is statistically significant when compared with the disease form of Htt. Consistent with our hypothesis that HDAC inhibition may act through modification of Htt, we found that the levels of Htt acetylation increased when HEK293 were cultured in the presence of HDAC inhibitors (trichostatin A, sodium butyrate, nicotinamide) (Fig. 5*B*). During this treatment the level of acetylation of Htt23Q when compared with Htt148Q was

normalized (Table III). Our results suggest HDAC treatment corrects altered acetylation levels between normal and the disease form of Htt.

DISCUSSION

As shown in Fig. 6, Htt is a very large protein with 3144 amino acids and the polyQ region is located at the N terminus. Proteolysis, localization, and clearance events for Htt play a key role in HD pathogenesis (10, 11, 20, 77). Htt is susceptible to proteolytic cleavage at Asp-513 and -552 by caspase-3/7, at Asp-586 by caspase-6 and at aspartic acid 552 by caspase-2 (Fig. 6*A*). The resulting N-terminal fragments are toxic (10, 78, 79). Htt is a substrate of calpains as well, cleaving at threonine Thr-469 and Ser-536 (11, 80). In addition, aspartyl endopeptidases cleave Htt within the amino acid region 104–114 (cpA) and 146–214 (cpB). The cpA fragments form nuclear aggregates (76, 77). Because the N-terminal 612 amino acids contain many of the proteolytic cleavage sites involved in the pathogenesis of HD (Fig. 6*B* summarizes the cascade) and contains the pathogenic polyQ stretch, we focused our study on the N-terminus and generated a construct containing the first 612 amino acids of Htt.

Acetylation has been recognized as a regulatory modification analogous to phosphorylation (27). Therefore, modification of mutant Htt acetylation is likely to control disease progression and toxicity analogous to that found for phosphorylation. Recent studies reveal that certain HDAC inhibitors have therapeutic results in HD transgenic mouse models (49, 81). In those studies, researchers focused on histone and attributed the neuroprotective effect to increased histone acetylation and resulting increased gene transcription. However, HDACs and HDAC inhibitors not only act on histones, but also on diverse range of proteins. Htt is one such candidate.

As summarized, five lysine acetylation sites were identified in our analysis. Among them, Lys-9 is in amino acids 1–17 of Htt flanking the polyQ tract (See Fig. 6). The first 17 amino acids of Htt modulate the cytoplasmic localization of Htt exon 1 protein (Httex1p), Htt aggregation and its effects on calcium homeostasis (74). Thompson *et al.* found acetylation of Lys-9 was detected on exogenous IKK overexpression and was regulated by phosphorylation of Ser-13 (82). Jeong *et al.* demonstrate that increased acetylation at Lys-444 facilitates trafficking of mutant Htt into autophagosomes and reduces the toxicity of mutant Htt (73). Post-translational modifications, including acetylation, can also effect Htt's interaction with associated proteins. The other three novel Htt acetyllysine sites (Lys-178, Lys-236, Lys-345) identified in our study reside either close to sites of proteolysis, protein interactions domains, or in the lipid-binding domain of Htt (75, 83). Therefore, they may have an impact on the cleavage of Htt or association of Htt with lipids.

The Htt lysine acetylation sites in this study were identified in cells expressing Htt23Q. A MRM-based quantitative study was conducted comparing the acetylation of Lys-178 in the wild type and mutant Htt. Our results indicate that wild-type Htt tends to be more acetylated at Lys-178 than the disease causing form of Htt. The site of acetylation is near the polyQ tract. Jeong *et al.* (74) demonstrated for Lys-444 that the acetylation levels are higher in mutant Htt when compared with wild-type using Western blot analysis with an antibody directed to the acetylated Lys-444 peptide. Our Western blot probed with a custom antibody for acetylated Lys-444 show similar trends for truncated mutant Htt proteins (Htt 1–612 and Htt 1–1212) consistent with this earlier study. The level of acetylation in the wild-type *versus* mutant Htt was not reported for the acetylation of Lys-9 (82). However, the Lys-9-acetylation regulating Ser-13 phosphorylation is more efficient for the wild type than for the expanded polyQ truncated Htt protein. Considering the relative positions of Lys-9, Lys-178, Lys-236, Lys-345, and Lys-444 to the N-terminus, and the polyQ region, there seems to be a pattern showing more wild-type Htt lysine acetylation at the N-terminal and/or close to the polyQ region. On the other hand, there is also a trend toward a higher level of lysine acetylation in mutant Htt at the C-terminus and/or away from the polyQ region.

In conclusion, our study confirmed that Htt is a highly acetylated protein and identified three novel acetylation sites. Further, we found quantitatively that the level of acetylation of mutant Htt was different than wild-type Htt. Consistent with our hypothesis that HDAC inhibition can directly target the disease protein, we found that HDAC inhibition corrected the altered levels of acetylation of mutant Htt relative to wild-type Htt. Given the increasing importance of acetylation in regulating neurodegenerative diseases, the new acetylation sites identified here will allow further functional exploration of the role of these PTMs in Huntington's disease.

Acknowledgment—We thank Dr. Yingming Zhao for advice on HDAC inhibitor treatment methods.

* This work was supported by the National Institutes of Health grants NS040251 (LME), NIH NS062413 (LME), CHDI (LME, BWG), and the Geroscience Mass Spectrometry and Imaging Core NIH PL1 AG032118 (BWG). The QSTAR Elite and 4000 QTRAP mass spectrometers were purchased through shared instrumentation grants from NCRR, S10RR024615 and S10 RR0021222 (BWG).

[S] This article contains supplemental Figs. S1 to S5 and Tables S1 to S5.

The data associated with this manuscript may be downloaded from ProteomeCommons.org Tranche using the following hash: cbC GqLS4LdE6fTbQUaAXE7xEHjxMHuJD2LA4/Qlwx4kdtiStouGLc 8ST9J99aClOamzoSaAhCLffLN7921AplGEEUMwAAAAAAAAhbQ

§ To whom correspondence should be addressed: Buck Institute for Research on Aging, 8001 Redwood Blvd, Novato, CA 94945. Tel.: (415) 209-2088; Fax: (415) 209-2230; E-mail: lellerby@buckinstitute.org.

REFERENCES

1. The Huntington's Disease Research Group, H. D. C. R. (1993) A novel gene containing a trinucleotide repeat that is expanded and unstable on Huntington's disease chromosomes. *Cell* **72,** 971–983
2. Vonsattel, J. P., Myers, R. H., Stevens, T. J., Ferrante, R. J., Bird, E. D., and

Richardson, E. P., Jr. (1985) Neuropathological classification of Huntington's disease. *J. Neuropathol. Exp. Neurol.* **44,** 559–577
3. Zuccato, C., Belyaev, N., Conforti, P., Ooi, L., Tartari, M., Papadimou, E., MacDonald, M., Fossale, E., Zeitlin, S., Buckley, N., and Cattaneo, E. (2007) Widespread disruption of repressor element-1 silencing transcription factor/neuron-restrictive silencer factor occupancy at its target genes in Huntington's disease. *J. Neurosci.* **27,** 6972–6983
4. Gafni, J., Hermel, E., Young, J. E., Wellington, C. L., Hayden, M. R., and Ellerby, L. M. (2004) Inhibition of calpain cleavage of huntingtin reduces toxicity: accumulation of calpain/caspase fragments in the nucleus. *J. Biol. Chem.* **279,** 20211–20220
5. Cha, J. H. (2000) Transcriptional dysregulation in Huntington's disease. *Trends Neurosci.* **23,** 387–392
6. Arrasate, M., Mitra, S., Schweitzer, E. S., Segal, M. R., and Finkbeiner, S. (2004) Inclusion body formation reduces levels of mutant huntingtin and the risk of neuronal death. *Nature* **431,** 805–810
7. Bae, B. I., Xu, H., Igarashi, S., Fujimuro, M., Agrawal, N., Taya, Y., Hayward, S. D., Moran, T. H., Montell, C., Ross, C. A., Snyder, S. H., and Sawa, A. (2005) p53 mediates cellular dysfunction and behavioral abnormalities in Huntington's disease. *Neuron* **47,** 29–41
8. Dunah, A. W., Jeong, H., Griffin, A., Kim, Y. M., Standaert, D. G., Hersch, S. M., Mouradian, M. M., Young, A. B., Tanese, N., and Krainc, D. (2002) Sp1 and TAFII130 transcriptional activity disrupted in early Huntington's disease. *Science* **296,** 2238–2243
9. Freiman, R. N., and Tjian R. (2002) Neurodegeneration. A glutamine-rich trail leads to transcription factors. *Science* **296,** 2149–2150
10. Graham, R. K., Deng, Y., Slow, E. J., Haigh, B., Bissada, N., Lu, G., Pearson, J., Shehadeh, J., Bertram, L., Murphy, Z., Warby, S. C., Doty, C. N., Roy, S., Wellington, C. L., Leavitt, B. R., Raymond, L. A., Nicholson, D. W., and Hayden, M. R. (2006) Cleavage at the caspase-6 site is required for neuronal dysfunction and degeneration due to mutant huntingtin. *Cell* **125,** 1179–1191
11. Kim, Y. J., Yi, Y., Sapp, E., Wang, Y., Cuiffo, B., Kegel, K. B., Qin, Z. H., Aronin, N., and DiFiglia, M. (2001) Caspase 3-cleaved N-terminal fragments of wild-type and mutant huntingtin are present in normal and Huntington's disease brains, associate with membranes, and undergo calpain-dependent proteolysis. *Proc. Natl. Acad. Sci. U.S.A.* **98,** 12784–12789
12. Chen-Plotkin, A. S., Sadri-Vakili, G., Yohrling, G. J., Braveman, M. W., Benn, C. L., Glajch, K. E., DiRocco, D. P., Farrell, L. A., Krainc, D., Gines, S., MacDonald, M. E., and Cha, J. H. (2006) Decreased association of the transcription factor Sp1 with genes downregulated in Huntington's disease. *Neurobiol. Dis.* **22,** 233–241
13. Cornett, J., Smith, L., Friedman, M., Shin, J. Y., Li, X. J., and Li, S. H. (2006) Context-dependent dysregulation of transcription by mutant huntingtin. *J. Biol. Chem.* **281,** 36198–36204
14. Rangone, H., Poizat, G., Troncoso, J., Ross, C. A., MacDonald, M. E., Saudou, F., and Humbert, S. (2004) The serum- and glucocorticoid-induced kinase SGK inhibits mutant huntingtin-induced toxicity by phosphorylating serine 421 of huntingtin. *Eur. J. Neurosci.* **19,** 273–279
15. Borrell-Pagès, M., Zala, D., Humbert, S., and Saudou, F. (2006) Huntington's disease: from huntingtin function and dysfunction to therapeutic strategies. *Cell Mol Life Sci* **63,** 2642–2660
16. Diaz-Hernández, M., Valera, A. G., Morán, M. A., Gómez-Ramos, P., Alvarez-Castelao, B., Castaño, J. G., Hernández, F., and Lucas, J. J. (2006) Inhibition of 26S proteasome activity by huntingtin filaments but not inclusion bodies isolated from mouse and human brain. *J. Neurochem.* **98,** 1585–1596
17. Dorval, V., and Fraser, P. E. (2007) SUMO on the road to neurodegeneration. *Biochim. Biophys. Acta* **1773,** 694–706
18. Saudou, F., Finkbeiner, S., Devys, D., and Greenberg, M. E. (1998) Huntingtin acts in the nucleus to induce apoptosis but death does not correlate with the formation of intranuclear inclusions. *Cell* **95,** 55–66
19. Humbert, S., Bryson, E. A., Cordelières, F. P., Connors, N. C., Datta, S. R., Finkbeiner, S., Greenberg, M. E., and Saudou, F. (2002) The IGF-1/Akt pathway is neuroprotective in Huntington's disease and involves Huntingtin phosphorylation by Akt. *Dev. Cell* **2,** 831–837
20. Schilling, B., Gafni, J., Torcassi, C., Cong, X., Row, R. H., LaFevre-Bernt, M. A., Cusack, M. P., Ratovitski, T., Hirschhorn, R., Ross, C. A., Gibson, B. W., and Ellerby, L. M. (2006) Huntingtin phosphorylation sites mapped by mass spectrometry. Modulation of cleavage and toxicity. *J. Biol. Chem.* **281,** 23686–23697
21. Luo, S., Vacher, C., Davies, J. E., and Rubinsztein, D. C. (2005) Cdk5 phosphorylation of huntingtin reduces its cleavage by caspases: implications for mutant huntingtin toxicity. *J. Cell Biol.* **169,** 647–656
22. Anne, S. L., Saudou, F., and Humbert, S. (2007) Phosphorylation of huntingtin by cyclin-dependent kinase 5 is induced by DNA damage and regulates wild-type and mutant huntingtin toxicity in neurons. *J. Neurosci.* **27,** 7318–7328
23. Steffan, J. S., Agrawal, N., Pallos, J., Rockabrand, E., Trotman, L. C., Slepko, N., Illes, K., Lukacsovich, T., Zhu, Y. Z., Cattaneo, E., Pandolfi, P. P., Thompson, L. M., and Marsh, J. L. (2004) SUMO modification of Huntingtin and Huntington's disease pathology. *Science* **304,** 100–104
24. Kalchman, M. A., Graham, R. K., Xia, G., Koide, H. B., Hodgson, J. G., Graham, K. C., Goldberg, Y. P., Gietz, R. D., Pickart, C. M., and Hayden, M. R. (1996) Huntingtin is ubiquitinated and interacts with a specific ubiquitin-conjugating enzyme. *J. Biol. Chem.* **271,** 19385–19394
25. Davie, J. R., and Spencer, V. A. Control of histone modifications. *J. Cell. Biochem.* Suppl 32–33:141–148, 1999
26. Spencer, V. A., and Davie, J. R. (1999) Role of covalent modifications of histones in regulating gene expression. *Gene* **240,** 1–12
27. Kouzarides, T. (2000) Acetylation: a regulatory modification to rival phosphorylation? *EMBO J.* **19,** 1176–1179
28. Yang, X. J., and Seto, E. (2007) HATs and HDACs: from structure, function and regulation to novel strategies for therapy and prevention. *Oncogene* **26,** 5310–5318
29. Kuo, M. H., and Allis, C. D. (1998) Roles of histone acetyltransferases and deacetylases in gene regulation. *Bioessays* **20,** 615–626
30. Shahbazian, M. D., and Grunstein, M. (2007) Functions of site-specific histone acetylation and deacetylation. *Annu. Rev. Biochem.* **76,** 75–100
31. Williams, S. K., Truong, D., and Tyler, J. K. (2008) Acetylation in the globular core of histone H3 on lysine-56 promotes chromatin disassembly during transcriptional activation. *Proc. Natl. Acad. Sci. U.S.A.* **105,** 9000–9005
32. Fu, M., Wang, C., Zhang, X., and Pestell, R. G. (2004) Acetylation of nuclear receptors in cellular growth and apoptosis. *Biochem. Pharmacol.* **68,** 1199–1208
33. Roh, M. S., Kim, C. W., Park, B. S., Kim, G. C., Jeong, J. H., Kwon, H. C., Suh, D. J., Cho, K. H., Yee, S. B., and Yoo, Y. H. (2004) Mechanism of histone deacetylase inhibitor Trichostatin A induced apoptosis in human osteosarcoma cells. *Apoptosis* **9,** 583–589
34. Balakin, K. V., Ivanenkov, Y. A., Kiselyov, A. S., and Tkachenko, S. E. (2007) Histone deacetylase inhibitors in cancer therapy: latest developments, trends and medicinal chemistry perspective. *Anticancer Agents Med. Chem.* **7,** 576–592
35. Zhang, J., Sprung, R., Pei, J., Tan, X., Kim, S., Zhu, H., Liu, C. F., Grishin, N. V., and Zhao, Y. (2009) Lysine acetylation is a highly abundant and evolutionarily conserved modification in Escherichia coli. *Mol. Cell Proteomics* **8,** 215–225
36. Aoki, E., and Schultz, R. M. (1999) DNA replication in the 1-cell mouse embryo: stimulatory effect of histone acetylation. *Zygote* **7,** 165–172
37. Chen, C. C., and Tyler, J. (2008) Chromatin reassembly signals the end of DNA repair. *Cell Cycle* **7,** 3792–3797
38. Chen, H., Schuster, M. C., Sfyroera, G., Geisbrecht, B. V., and Lambris, J. D. (2008) Solution insights into the structure of the Efb/C3 complement inhibitory complex as revealed by lysine acetylation and mass spectrometry. *J. Am. Soc. Mass Spectrom.* **19,** 55–65
39. Escargueil, A. E., Soares, D. G., Salvador, M., Larsen, A. K., and Henriques, J. A. (2008) What histone code for DNA repair? *Mutat. Res.* **658,** 259–270
40. Block-Galarza, J., Chase, K. O., Sapp, E., Vaughn, K. T., Vallee, R. B., DiFiglia, M., and Aronin, N. (1997) Fast transport and retrograde movement of huntingtin and HAP 1 in axons. *Neuroreport* **8,** 2247–2251
41. Huen, M. S., and Chen, J. (2008) The DNA damage response pathways: at the crossroad of protein modifications. *Cell Res.* **18,** 8–16
42. Borchers, A., Braspenning, J., Meijer, J., Osen, W., Gissmann, L., and Jochmus, I. (1999) E7-specific cytotoxic T cell tolerance in HPV-transgenic mice. *Arch. Virol.* **144,** 1539–1556
43. Muftuoglu, M., Kusumoto, R., Speina, E., Beck, G., Cheng, W. H., and Bohr, V. A. (2008) Acetylation regulates WRN catalytic activities and affects base excision DNA repair. *PLoS ONE* **3,** e1918
44. O'Connor, M. J., Martin, N. M., and Smith, G. C. (2007) Targeted cancer therapies based on the inhibition of DNA strand break repair. *Oncogene* **26,** 7816–7824

45. Chiang, M. C., Chen, H. M., Lee, Y. H., Chang, H. H., Wu, Y. C., Soong, B. W., Chen, C. M., Wu, Y. R., Liu, C. S., Niu, D. M., Wu, J. Y., Chen, Y. T., and Chern, Y. (2007) Dysregulation of C/EBPalpha by mutant Huntingtin causes the urea cycle deficiency in Huntington's disease. *Hum. Mol. Genet.* **16,** 483–498
46. Kim, S. C., Sprung, R., Chen, Y., Xu, Y., Ball, H., Pei, J., Cheng, T., Kho, Y., Xiao, H., Xiao, L., Grishin, N. V., White, M., Yang, X. J., and Zhao, Y. (2006) Substrate and functional diversity of lysine acetylation revealed by a proteomics survey. *Mol. Cell* **23,** 607–618
47. Monti, B., Gatta, V., Piretti, F., Raffaelli, S. S., Virgili, M., and Contestabile, A. (Valproic acid is neuroprotective in the rotenone rat model of Parkinson's disease: involvement of alpha-synuclein. *Neurotox. Res.* **17,** 130–141
48. Kilgore, M., Miller, C. A., Fass, D. M., Hennig, K. M., Haggarty, S. J., Sweatt, J. D., and Rumbaugh, G. (Inhibitors of class 1 histone deacetylases reverse contextual memory deficits in a mouse model of Alzheimer's disease. *Neuropsychopharmacology* **35,** 870–880
49. Hockly, E., Richon, V. M., Woodman, B., Smith, D. L., Zhou, X., Rosa, E., Sathasivam, K., Ghazi-Noori, S., Mahal, A., Lowden, P. A., Steffan, J. S., Marsh, J. L., Thompson, L. M., Lewis, C. M., Marks, P. A., and Bates, G. P. (2003) Suberoylanilide hydroxamic acid, a histone deacetylase inhibitor, ameliorates motor deficits in a mouse model of Huntington's disease. *Proc. Natl. Acad. Sci. U.S.A.* **100,** 2041–2046
50. Ferrante, R. J., Kubilus, J. K., Lee, J., Ryu, H., Beesen, A., Zucker, B., Smith, K., Kowall, N. W., Ratan, R. R., Luthi-Carter, R., and Hersch, S. M. (2003) Histone deacetylase inhibition by sodium butyrate chemotherapy ameliorates the neurodegenerative phenotype in Huntington's disease mice. *J. Neurosci.* **23,** 9418–9427
51. Feng, H. L., Leng, Y., Ma, C. H., Zhang, J., Ren, M., and Chuang, D. M. (2008) Combined lithium and valproate treatment delays disease onset, reduces neurological deficits and prolongs survival in an amyotrophic lateral sclerosis mouse model. *Neuroscience* **155,** 567–572
52. Butler, R., and Bates, G. P. (2006) Histone deacetylase inhibitors as therapeutics for polyglutamine disorders. *Nat. Rev. Neurosci.* **7,** 784–796
53. Bridges, K. R., Schmidt, G. J., Jensen, M., Cerami, A., and Bunn, H. F. (1975) The acetylation of hemoglobin by aspirin. In vitro and in vivo. *J. Clin. Invest.* **56,** 201–207
54. Schmitt, M., and Matthies, H. (1979) [Biochemical studies on histones of the central nervous system. I. Characterization and partial identification of the label of histones from rat brain following intraventricular administration of 1-[14C]-acetate]. *Acta Biol. Med. Ger.* **38,** 673–676
55. Qiang, L., Xiao, H., Campos, E. I., Ho, V. C., and Li, G. (2005) Development of a PAN-specific, affinity-purified anti-acetylated lysine antibody for detection, identification, isolation, and intracellular localization of acetylated protein. *J. Immunoassay Immunochem.* **26,** 13–23
56. Chen, L. F., and Greene, W. C. (2005) Assessing acetylation of NF-kappaB. *Methods* **36,** 368–375
57. Kouach, M., Belaïche, D., Jaquinod, M., Couppez, M., Kmiecik, D., Ricart, G., Van Dorsselaer, A., Sautière, P., and Briand, G. (1994) Application of electrospray and fast atom bombardment mass spectrometry to the identification of post-translational and other chemical modifications of proteins and peptides. *Biol. Mass Spectrom.* **23,** 283–294
58. Wilm, M., Shevchenko, A., Houthaeve, T., Breit, S., Schweigerer, L., and Fotsis, T., Mann, M. (1996) Femtomole sequencing of proteins from polyacrylamide gels by nano-electrospray mass spectrometry. *Nature* **379,** 466–469
59. Siuti, N., and Kelleher, N. L. (2007) Decoding protein modifications using top-down mass spectrometry. *Nat. Methods* **4,** 817–821
60. Loo, J., andLoo, R. R. O. (1997) *Electrospray Ionization Mass Spectrometry,* ed Cole, R. B. (John Wiley, New York), pp 385–419
61. Winston, R., and Fitzgerald, M. (1996) Mass spectrometry as a readout of protein structure and function *Mass Spectrometry Rev.* **379,** 466–469
62. Witze, E. S., Old, W. M., Resing, K. A., and Ahn, N. G. (2007) Mapping protein post-translational modifications with mass spectrometry. *Nat. Methods* **4,** 798–806
63. Choudhary, C., Kumar, C., Gnad, F., Nielsen, M. L., Rehman, M., Walther, T. C., Olsen, J. V., and Mann, M. (2009) Lysine acetylation targets protein complexes and co-regulates major cellular functions. *Science* **325,** 834–840
64. Falick, A. M., Hines, W. M., Medzihradszky, K. F., Baldwin, M. A., and Gibson, B. W. (1993) Low-mass ions produced from peptides by high-energy collision-induced dissociation in tandem mass spectrometry *J. Am. Soc. Mass Spectrom.* **4,** 882–893
65. Borchers, M. T., Wesselkamper, S., Wert, S. E., Shapiro, S. D., and Leikauf, G. D. (1999) Monocyte inflammation augments acrolein-induced Muc5ac expression in mouse lung. *Am. J. Physiol.* **277,** L489–497
66. Schilling, B., Row, R. H., Gibson, B. W., Guo, X., and Young, M. M. (2003) MS2Assign, automated assignment and nomenclature of tandem mass spectra of chemically crosslinked peptides. *J. Am. Soc. Mass Spectrom.* **14,** 834–850
67. Chen, R., Fearnley, I. M., Palmer, D. N., and Walker, J. E. (2004) Lysine 43 is trimethylated in subunit C from bovine mitochondrial ATP synthase and in storage bodies associated with batten disease. *J. Biol. Chem.* **279,** 21883–21887
68. Zhang, K., Williams, K. E., Huang, L., Yau, P., Siino, J. S., Bradbury, E. M., Jones, P. R., Minch, M. J., and Burlingame, A. L. (2002) Histone acetylation and deacetylation: identification of acetylation and methylation sites of HeLa histone H4 by mass spectrometry. *Mol. Cell Proteomics* **1,** 500–508
69. Cocklin, R. R., and Wang, M. (2003) Identification of methylation and acetylation sites on mouse histone H3 using matrix-assisted laser desorption/ionization time-of-flight and nanoelectrospray ionization tandem mass spectrometry. *J. Protein Chem.* **22,** 327–334
70. Chen, C., Zhou, Z., Guo, P., and Dong, J. T. (2007) Proteasomal degradation of the KLF5 transcription factor through a ubiquitin-independent pathway. *FEBS Lett.* **581,** 1124–1130
71. Dormeyer, W., Ott, M., and Schnölzer, M. (2005) Probing lysine acetylation in proteins: strategies, limitations, and pitfalls of in vitro acetyltransferase assays. *Mol. Cell Proteomics* **4,** 1226–1239
72. Perkins, D. N., Pappin, D. J., Creasy, D. M., and Cottrell, J. S. (1999) Probability-based protein identification by searching sequence databases using mass spectrometry data. *Electrophoresis* **20,** 3551–3567
73. Stevens, S. M., Jr., Prokai-Tatrai, K., and Prokai, L. (2008) Factors that contribute to the misidentification of tyrosine nitration by shotgun proteomics. *Mol. Cell Proteomics* **7,** 2442–2451
74. Jeong, H., Then, F., Melia, T. J., Jr., Mazzulli, J. R., Cui, L., Savas, J. N., Voisine, C., Paganetti, P., Tanese, N., Hart, A. C., Yamamoto, A., and Krainc, D. (2009) Acetylation targets mutant huntingtin to autophagosomes for degradation. *Cell* **137,** 60–72
75. Rockabrand, E., Slepko, N., Pantalone, A., Nukala, V. N., Kazantsev, A., Marsh, J. L., Sullivan, P. G., Steffan, J. S., Sensi, S. L., and Thompson, L. M. (2007) The first 17 amino acids of Huntingtin modulate its subcellular localization, aggregation and effects on calcium homeostasis. *Hum. Mol. Genet.* **16,** 61–77
76. Ratovitski, T., Gucek, M., Jiang, H., Chighladze, E., Waldron, E., D'Ambola, J., Hou, Z., Liang, Y., Poirier, M. A., Hirschhorn, R. R., Graham, R., Hayden, M. R., Cole, R. N., and Ross, C. A. (2009) Mutant huntingtin N-terminal fragments of specific size mediate aggregation and toxicity in neuronal cells. *J. Biol. Chem.* **284,** 10855–10867
77. Lunkes, A., Lindenberg, K. S., Ben-Haïem, L., Weber, C., Devys, D., Landwehrmeyer, G. B., Mandel, J. L., and Trottier, Y. (2002) Proteases acting on mutant huntingtin generate cleaved products that differentially build up cytoplasmic and nuclear inclusions. *Mol. Cell* **10,** 259–269
78. Wellington, C. L., Ellerby, L. M., Gutekunst, C. A., Rogers, D., Warby, S., Graham, R. K., Loubser, O., van Raamsdonk, J., Singaraja, R., Yang, Y. Z., Gafni, J., Bredesen, D., Hersch, S. M., Leavitt, B. R., Roy, S., Nicholson, D. W., and Hayden, M. R. (2002) Caspase cleavage of mutant huntingtin precedes neurodegeneration in Huntington's disease. *J. Neurosci.* **22,** 7862–7872
79. Wellington, C. L., Singaraja, R., Ellerby, L., Savill, J., Roy, S., Leavitt, B., Cattaneo, E., Hackam, A., Sharp, A., Thornberry, N., Nicholson, D. W., Bredesen, D. E., and Hayden, M. R. (2000) Inhibiting caspase cleavage of huntingtin reduces toxicity and aggregate formation in neuronal and nonneuronal cells. *J. Biol. Chem.* **275,** 19831–19838
80. Gafni, J., and Ellerby, L. M. (2002) Calpain activation in Huntington's disease. *J. Neurosci.* **22,** 4842–4849
81. Gardian, G., Browne, S. E., Choi, D. K., Klivenyi, P., Gregorio, J., Kubilus, J. K., Ryu, H., Langley, B., Ratan, R. R., Ferrante, R. J., and Beal, M. F. (2005) Neuroprotective effects of phenylbutyrate in the N171–82Q transgenic mouse model of Huntington's disease. *J. Biol. Chem.* **280,** 556–563

82. Thompson, L. M., Aiken, C. T., Kaltenbach, L. S., Agrawal, N., Illes, K., Khoshnan, A., Martinez-Vincente, M., Arrasate, M., O'Rourke, J. G., Khashwji, H., Lukacsovich, T., Zhu, Y. Z., Lau, A. L., Massey, A., Hayden, M. R., Zeitlin, S. O., Finkbeiner, S., Green, K. N., LaFerla, F. M., Bates, G., Huang, L., Patterson, P. H., Lo, D. C., Cuervo, A. M., Marsh, J. L., and Steffan, J. S. (2009) IKK phosphorylates Huntingtin and targets it for degradation by the proteasome and lysosome. *J. Cell Biol.* **187,** 1083–1099
83. Kegel, K. B., Sapp, E., Yoder, J., Cuiffo, B., Sobin, L., Kim, Y. J., Qin, Z. H., Hayden, M. R., Aronin, N., Scott, D. L., Isenberg, G., Goldmann, W. H., and DiFiglia, M. (2005) Huntingtin associates with acidic phospholipids at the plasma membrane. *J. Biol. Chem.* **280,** 36464–36473
84. DiFiglia, M., Sena-Esteves, M., Chase, K., Sapp, E., Pfister, E., Sass, M., Yoder, J., Reeves, P., Pandey, R. K., Rajeev, K. G., Manoharan, M., Sah, D. W., Zamore, P. D., and Aronin, N. (2007) Therapeutic silencing of mutant huntingtin with siRNA attenuates striatal and cortical neuropathology and behavioral deficits. *Proc. Natl. Acad. Sci. U.S.A.* **104,** 17204–17209

In order to cite this article properly, please include all of the following information: Cong, X., Held, J. M., DeGiacomo, F., Bonner, A., Chen, J. M., Schilling, B., Czerwieniec, G. A., Gibson, B. W., and Ellerby, L. M. (2011) Mass Spectrometric Identification of Novel Lysine Acetylation Sites in Huntingtin. *Mol. Cell. Proteomics* 10(10):M111.009829. DOI: 10.1074/mcp.M111.009829.